ACTA ACUSTICA UNITED WITH ACUSTICA
Vol. 88 (2002) 827 – 836

Sound Transmission Through a Plate by an Energy Flow Approach

V. Cotoni, A. Le Bot, L. Jezequel
Laboratoire de Tribologie et Dynamique des Systèmes, École Centrale de Lyon, 36, Avenue Guy de Collongues 69131 BP163 Écully, France. e-mail: vincent.cotoni@gaus.gme.usherb.ca

Summary
The transmission of a plane sound wave through a finite plate is investigated by means of a local energy approach. This study is an extension to vibroacoustic problems of an integral energy approach dedicated to the high frequencies. This approximate approach deals with energy density and intensity, and leads to the spatial distribution of energy averaged over time and frequency. Both resonant and non-resonant transmission processes are considered, below and above the critical frequency of the fluid-loaded plate. This paper focusses on the sound transmission between two semi-infinite acoustical media, giving rise to non diffuse pressure fields. Both structural and acoustic averaged energy fields are well described except on caustics.

PACS no. 43.20.Tb

1. Introduction

The transmission of sound through walls has been studied for a long time and complex phenomena have been highlighted, even in the simple case of the transmission of a plane wave through a finite thin plate [1, 2]. For the description of such vibroacoustic systems in the higher part of the audio frequency band, classical approaches like finite or boundary element methods are not relevant due to the high computation cost. As a solution, statistical approaches dedicated to high frequencies and based on energy quantities have been developed. The most famous one, the Statistical Energy Analysis (SEA), solves systems by applying a global power balance for each subsystem [2, 3], assuming that energy fields are diffuse. The total averaged-energy of each subsystem is thus obtained.

As an alternative to SEA, the energy flow approach described in this paper is based on some local energy quantities so that the distribution of energy inside the subsystems is available. It has already been applied to pure acoustical problems [4, 5, 6], to the coupling between structures and cavities [7], and to pure radiation problems [8]. It is here investigated for the transmission between two semi-infinite acoustical media, which corresponds to a problem where energy fields are not diffuse at all. The present approach is based on a simplified analysis: this involves power balance in which the incident field excites the plate, plate vibrations dissipate energy and plate vibrations radiate energy. By virtue of the locality principle valid at high frequencies [9], the power balance for excitation and radiation processes are derived by solving some local canonical problems. As a result, the radiation is approximated by the relevant edge/surface radiation from semi-infinite/infinite plates, the expression depending on whether the excitation is below or above the coincidence frequency.

The successive steps of the calculation are detailed as follows. In section 2, energy fields corresponding to some elementary waves are briefly studied. They are then used in both the structural and acoustic energy formulations to describe the contribution of some power sources introduced on boundaries to check the energy flow balance at couplings. In section 3, the corresponding power balance equations at couplings are derived by solving some canonical problems involving resonant and non-resonant transmission effects. The resolution of the whole vibroacoustic system is then performed in section 4 and some numerical comparisons with reference results are presented in section 5.

For the sake of simplicity, the transmission problem is reduced to a two-dimensional system by considering a one-dimensional baffled structure excited by a plane sound wave. This paper focusses on the distributions of flexural energy in the structure and transmitted sound energy.

2. Description of energy fields

2.1. Energy fields for plane and cylindrical waves

We note G and $\mathbf{H}$ the time-averaged energy density and intensity vector due to a traveling plane or cylindrical damped wave, in steady state conditions at pulsation ω. The local power balance is written [5],

$$\operatorname{div} \mathbf{H} + \eta\omega G = \delta(S), \tag{1}$$

Received 24 January 2001,
accepted 11 February 2002.

where η is the loss factor assumed to be light ($\eta \ll 1$), and S the point source. The dissipated power is taken to be $\eta\omega G$ i.e. proportional to the energy density. This relationship is rather conventional in the high frequency literature [3] although it requires some comments. In acoustics this relationship may be considered as relevant for the atmospheric absorption in far-field. In structural dynamics, the underlying assumption is that potential energy and kinetic energy are equal so that the dissipated power may be expressed in terms of the total energy density, the damping process being viscous or hysteretic. Indeed, this is not true in a strictly sense but is generally considered as valid for local quantities averaged over time, frequency and space, except in some special cases like the non-resonant field in an acoustically excited structure. Furthermore, the condition that the wave propagates is embodied in the relation

$$\mathbf{H} = c\, G\, \mathbf{u}, \tag{2}$$

where $\mathbf{u}$ is the unit vector in the direction of propagation and c the group speed of the wave. Substituting equation (2) in equation (1), solutions for G and $\mathbf{H}$ at any point M are derived as

$$G(S,M) = \frac{1}{c}\frac{\mathrm{e}^{-\eta\omega r/c}}{\gamma_0\, r^{n-1}} \tag{3}$$

$$\text{and} \qquad \mathbf{H}(S,M) = \frac{\mathrm{e}^{-\eta\omega r/c}}{\gamma_0\, r^{n-1}}\, \mathbf{u}_{SM},$$

where $r = |SM|$ and $\mathbf{u}_{SM}$ is the unit vector in the direction from the source point S to the receiving point M. $n = 1$, $\gamma_0 = 2$ for plane waves and $n = 2$, $\gamma_0 = 2\pi$ for cylindrical waves. These expressions will be used to derive the energy contribution of the boundary sources involved in the description of the structural and acoustic energy fields.

2.2. Decomposition of systems

Consider the baffled structure of Figure 1 excited by an incoming plane sound wave carrying the intensity I_a^{inc}.

In order to predict the whole structural and acoustic averaged energy fields, these fields are split into several waves of type described above. Some future sources are introduced on the boundaries of the subsystems to check the local power balances. Further, the assumption is made that all waves are uncorrelated so that their energy contributions may be simply summed. Indeed, the choice of decomposition of energy fields into traveling waves is of great importance and, in general, different decompositions will lead to different results. The leading idea is that the decomposition must be as more "physical" as possible and that energy balance must always be verified. The structural and acoustic fields are split up as follows.

The energy W_s on the structure is thought of as the superposition of the forced term W_0 due to the incoming sound wave and the free term W_f due to waves traveling in the structure [1]. By virtue of the uncorrelation assumption, both energy contributions are simply summed and the total energy is written $W_s = W_0 + W_f$. In order to check

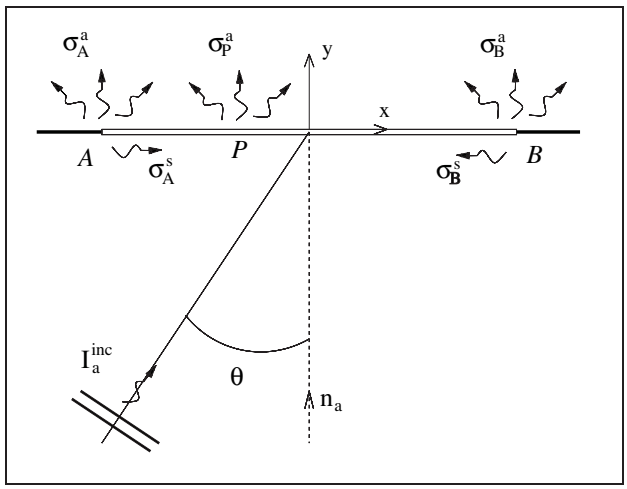

Figure 1. Sound transmission through a baffled plate: two structural sources, σ_A^s and σ_B^s describe the structural free energy W_f. Two point acoustic sources, σ_A^a and σ_B^a, and a density of acoustic sources, σ_P^a are introduced to describe the transmitted sound energy W_a.

the power balance on extremities A and B of the structure, two boundary sources, σ_A^s and σ_B^s are introduced (see Figure 1). The resulting free energy W_f and intensity $\mathbf{I}_f$ are written for any point P on the structure

$$\begin{cases} W_f(P) = \sigma_A^s\, G_p(A,P) + \sigma_B^s\, G_p(B,P), \\ \mathbf{I}_f(P) = \sigma_A^s\, \mathbf{H}_p(A,P) + \sigma_B^s\, \mathbf{H}_p(B,P). \end{cases} \tag{4}$$

G_p and $\mathbf{H}_p$ are the solutions given in equations (3) for plane waves.

The transmitted sound energy is described by two point sources, σ_A^a and σ_B^a located on extremities A and B, and by a density of boundary sources, σ_P^a (see Figure 1). The reasons why the sources are located on extremities and distributed on the whole surface will become clear in the next section dealing with canonical problems. We must consider that these sources σ_X^a where $X = A, B, P$ depend on the emission direction. The sound energy is written at any point M,

$$W_a(M) = \sigma_A^a(\varphi_{AM})\, G_c(A,M) + \sigma_B^a(\varphi_{BM})\, G_c(B,M) + \int_{AB} \sigma_P^a(\varphi_{PM})\, G_p(P,M)\, \mathrm{d}\varphi_{PM}, \tag{5}$$

with G_c being the energy solution (3) for cylindrical waves. φ_{PM} denotes the angle between the normal to the plate $\mathbf{n}_a$ and the direction from the point P to the point M.

Some canonical problems are now considered in order to derive the magnitudes $\sigma_{A,B}^s$, $\sigma_{A,B}^a$ and σ_P^a of the structural and acoustic boundary sources. The structural forced energy field W_0 is also evaluated. At this stage, the locality principle which states that the dynamics of a coupling only depends on the local characteristics of the coupling is invoked. The canonical problems are consequently not derived with the actual configuration of the vibroacoustic

system but with infinite or semi-infinite configurations that lead to much more simpler resolutions.

3. Canonical problems

Several processes are involved in the transmission of sound through thin elastic plates. They may be divided into resonant and non-resonant effects [1, 2]. The resonant transmission corresponds to the radiation of free flexural waves traveling in the structure while the non-resonant transmission is due to acoustically-forced waves in the structure. These aspects are detailed below with the resolution of some canonical problems in terms of power balance. In each case, both the magnitude and the directivity of the power sources involved in the problem are determined. For the sake of clarity, details of calculations are reported in Appendix.

3.1. Non-resonant transmission

Consider an infinite plate excited by a plane sound wave incident with the angle θ (Figure 2).

Some plane sound waves are reflected and transmitted through the plate and a flexural plane wave is created so that this canonical problem is related to the distributed acoustic sources σ_P^a and the forced structural energy W_0. The ratios of reflected and transmitted powers P_{refl}, P_{tran} over the incident one P_{inc} are written Σ_{nr}^1 and Σ_{nr}^2 (see expressions (A1) in Appendix). The corresponding emission angles, noted φ_{nr}^1 and φ_{nr}^2, are given in equations (A2). The structural energy W_0 in equation (A5) is that of the forced wave. The power balance states the equality of the incident power, i.e. the flux of the incident intensity over the plate, with the reflected, transmitted and dissipated powers, $P_{inc} = P_{refl} + P_{tran} + P_{diss}$. The power being dissipated is due to internal damping in the structure, taken into account by the loss factor η. It is shown in equation (A6) to be proportional to the incident sound power, $P_{diss} = \Sigma_{nr}^{diss} P_{inc}$, so that the global power balance can be expressed independently on the amount of incident power:

$$\Sigma_{nr}^1 + \Sigma_{nr}^2 + \Sigma_{nr}^{diss} = 1. \tag{6}$$

This equation shows that all the power transmitted to the structure is used to produce the forced wave which may induce energy losses if the structure is damped. If the structure is undamped, $\Sigma_{nr}^{diss} = 0$ and all the incident power is reflected and transmitted. Since the forced energy is taken into account by the term W_0, no structural power source needs to be introduced along the structure. The plane shape of the transmitted sound wave and the location of the non-resonant transmission phenomenon justify the introduction of the acoustic power sources σ_P^a in equation (5) distributed along the whole structure, and the use of the energy solution (3) for plane waves to describe their contribution to the acoustic energy. This implementation is detailed in section 4.

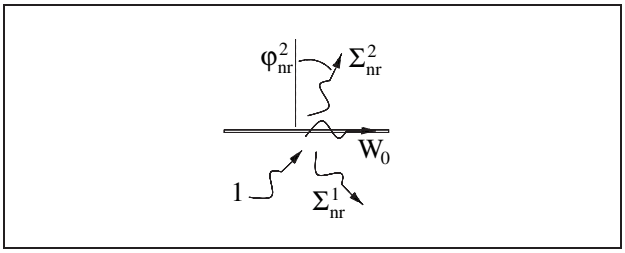

Figure 2. Canonical problem for non-resonant transmission.

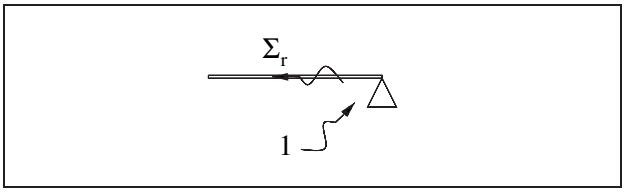

Figure 3. Canonical problem for structure excitation.

3.2. Resonant transmission

The resonant transmission process may be divided in two steps. The structure is first excited by the incoming sound wave. The resultant free structural field then radiates in both acoustical media [1].

3.2.1. Excitation of structures

Consider a semi-infinite plate excited by a plane sound wave incident with the angle θ (Figure 3).

Compared to the previous canonical problem, the plate is now bounded so that a free flexural field is created. The aim of this canonical calculation is to determine the power being supplied to the plate, then leading to the structural sources $\sigma_{A,B}^s$. The ratio of structural power emanating from the edge of the plate over the incident sound power is noted Σ_r in equation (A8). It is clear from the comparison of this canonical problem with the previous one that the free wave emanates from the edge of the plate. The exchange of power from the incident sound wave to the plate is thus confined at the edge. This is the reason why in equation (4) the free structural field is the sum of only two terms $\sigma_{A,B}^s$ and no distributed source was added. Due to the simplifications made for the solving of the canonical problem in Appendix, one only knows the ratio Σ_r of structural power P_s over the incident sound power P_{inc}. Rigorously, some reflected, transmitted and diffracted sound intensities are also to be evaluated. They have been omitted and the local power balance reduces to

$$P_s = \Sigma_r P_{inc}. \tag{7}$$

It should be added that the local power balance (6) valid for the transmission through an infinite plate no longer applies in the vicinity of the edge, due to the parts of the sound power transmitted to the structure and diffracted by the edge. Therefore, at the edge in the directions φ_{nr}^1 and φ_{nr}^2 of non-resonant transmission/reflection, the non-resonant transmission/reflection efficiencies Σ_{nr}^1 and Σ_{nr}^2

need to be modified. These directions correspond to caustics. In the vicinity of these lines, the pressure may not be thought of as the superposition of plane and cylindrical waves [9] so that our simple decomposition does not apply. However that may be, we shall consider in the present asymptotic analysis, that equality (6) always applies, meaning that the estimated sound intensity in the caustics directions is wrong. As a consequence, the description of the energy field is right everywhere except in the vicinity of caustics. This is an important limitation of the present method.

3.2.2. Radiation of structures

Two mechanisms are involved in the radiation of the structure.

The scattering of flexural waves on structural discontinuities occurs at any frequency [10]. In the present problem, it appears on extremities of the plate and is usually called edge radiation [11]. The point acoustic sources $\sigma^a_{A,B}$ are introduced in equation (5) to account for this phenomenon. The canonical calculation is performed with a baffled semi-infinite plate with a flexural wave impinging on the boundary (Figure 4).

Part of the incident power is reflected in the structure, the other part is diffracted in both acoustical media. The ratio of reflected power over the incident one is noted R in equation (A13). The diffracted sound wave is shown to be cylindrical centered on the edge point. The ratio of the radiated power per unit solid angle about direction φ, over the incident flexural power is written $\Sigma^i_e(\varphi)$ in equation (A12), where φ denotes the angle with the normal to the plate. The power balance for the system states the equality of the reflected and radiated powers with the incident one,

$$R + \int_{-\pi/2}^{\pi/2} \Sigma^1_e(\varphi)\,\mathrm{d}\varphi + \int_{-\pi/2}^{\pi/2} \Sigma^2_e(\varphi)\,\mathrm{d}\varphi = 1. \quad (8)$$

Since the radiated waves are cylindrical centered on the extremity point, the resulting power sources $\sigma^a_{A,B}$ in equation (5) are located on both extremities of the structure and the energy solution (3) for cylindrical waves is used to describe their contribution to the acoustic energy.

The second radiation process occurs during the propagation of the free flexural waves (Figure 5).

It appears above the so-called critical frequency when flexural waves become supersonic, and corresponds to the surface radiation process [11]. This phenomenon is consequently related to the distributed acoustic source σ^a_P. A plane sound waves is radiated in each media in directions φ^1_s and φ^2_s given in equation (A14). The ratio of power being radiated in the medium i over the power carried by the flexural wave is noted Σ^i_s in equation (A15). The resulting attenuation of the flexural wave is described with the radiation loss factor

$$\eta_s = c_s(\Sigma^1_s + \Sigma^2_s)/\omega \quad (9)$$

to be added to the damping loss factor η in expressions (3). c_s denotes the group speed of the flexural wave. Thus,

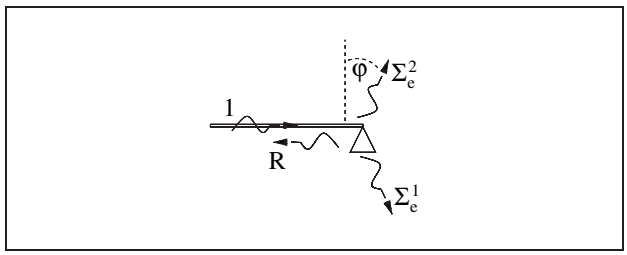

Figure 4. Canonical problem for edge radiation.

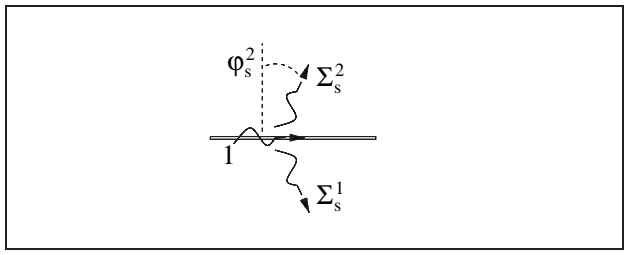

Figure 5. Canonical problem for surface radiation.

above the critical frequency, each free wave traveling in the plate is subjected to this radiation process and therefore, must be described with energy solutions (3) including the additional radiation loss factor (9). The power sources σ^a_P describing the radiation of the supersonic waves in equation (5) are distributed along the structure, with the directivity $\pm\varphi^1_s$ depending on the direction of propagation of the flexural wave. Energy solutions (3) for plane waves in acoustics are used for their contribution to the acoustic energy. When flexural waves are subsonic, no power is radiated by this process since only evanescent waves are created in the acoustical medium.

Above the critical frequency, both radiation processes occur giving rise to caustics starting from both extremities A and B with the angles $\pm\varphi^1_s$ and $\pm\varphi^2_s$. The same problem as encountered for the excitation of structures in subsection 3.2.1 also appears so that the description of energy will be realistic except near these caustics. Similarly the power balance (8) does not apply since efficiencies Σ^i_e need to be modified in the directions of caustics $\pm\varphi^i_s$. In fact, the efficiencies evaluated by solving the previous canonical problem do not verify the power balance because they have some strong singularities in the directions $\pm\varphi^i_s$. Integrals of equation (8) are therefore singular and the reflection coefficient R for the fluid-loaded plate can not be derived. A convenient way to overcome this difficulty is to consider that $R = 1$ when solving the structural problem. Indeed an error is introduced since the structure seems to not loss some energy by edge diffraction. But this error is expected to be relatively light, the largest part of energy being exchanged by surface radiation process [2, 11]. But when solving the acoustical problem, the singular efficiencies are applied separately for each direction excepted for caustics directions. The acoustic energy is thus correct far from the caustics.

4. Resolution of the system

The system resolution requires the calculation of all the boundary sources $\sigma^s_{A,B}$, $\sigma^a_{A,B}$ and σ^a_P shown in Figure 1. To this aim, the local power balances derived in the previous canonical problems are written in terms of the power sources of equations (4,5) and the energy solutions of equation (3). The two structural sources σ^s_A and σ^s_B are first determined. The resonant excitation and the radiation by edge scattering are involved in the energy behavior at edges A and B, and the corresponding canonical problems are invoked. The power balance on each extremities states that the structural power emanating from the edge is related to the incident sound power I^{inc}_a and to the structural power coming from the opposite edge by equalities,

$$\begin{cases} \frac{1}{2}\sigma^s_A = \Sigma_r\, \mathbf{I}^{inc}_a \mathbf{n}_a + R\,[\sigma^s_B\, \mathbf{H}_p(B,A).\mathbf{n}_{s,A}], \\ \frac{1}{2}\sigma^s_B = \Sigma_r\, \mathbf{I}^{inc}_a \mathbf{n}_a + R\,[\sigma^s_A\, \mathbf{H}_p(A,B).\mathbf{n}_{s,B}]. \end{cases} \tag{10}$$

R and Σ_r are defined in the previous canonical calculations. $\mathbf{I}^{inc}_a$ is the intensity of the incident sound wave, and $\mathbf{n}_a$ is the unit vector normal to the plate. $\mathbf{H}_p$ denotes the solution (3) for plane waves, taking into account the radiation loss (9) when flexural waves are supersonic. $\mathbf{n}_{s,A}$ and $\mathbf{n}_{s,B}$ are unit vectors oriented outside the plate from its extremities. The terms inside brackets are the incoming flexural energy flow on both extremities, which are reflected with the coefficient R. The contribution of the energy flow of the forced waves does not appear since it is included in the term Σ_r. The two solutions σ^s_A and σ^s_B of this system are introduced in equation (4) to evaluate the flexural energy density W_f related to the free waves.

The acoustic sources σ^a_A, σ^a_B, and the density of acoustic sources, σ^a_P are now evaluated. At any point P of the structure except extremities A and B, the emitted power is written as the sum of the radiated power from the supersonic flexural waves and the transmitted power by non-resonant process. Furthermore, the intensity into direction φ is $\sigma^a_P(\varphi)\mathbf{u}(\varphi)/2$ where $\mathbf{u}(\varphi)$ is the unit vector in direction defined by φ. The emitted power is thus $P_{rad} = \sigma^a_P(\varphi)\cos(\varphi)/2$, and is written according to the relevant canonical solutions,

$$\begin{aligned} \sigma^a_P(\varphi)\frac{\cos\varphi}{2} \;=\; & \Sigma^2_s\,[\sigma^s_A\, \mathbf{H}_p(A,P)\mathbf{n}_{s,B}]\,\delta(\varphi-\varphi^2_s) \\ & +\Sigma^2_s\,[\sigma^s_B\, \mathbf{H}_p(B,P)\mathbf{n}_{s,A}]\,\delta(\varphi+\varphi^2_s) \\ & +\Sigma^2_{nr}\,\mathbf{I}^{inc}_a \mathbf{n}_a\,\delta(\varphi-\varphi^2_{nr}). \end{aligned} \tag{11}$$

The first two terms describe the supersonic flexural waves radiation and are to be considered above the critical frequency only. Each term is related to a direction of propagation on the structure: quantities inside brackets are the flexural energy flow traveling in the corresponding direction, at the point P. The last term describes the non-resonant transmission. The singular directivities of each radiation process are taken into account by the Dirac terms.

On structure extremities, the edge radiation must be taken into account in addition to expression (11). The two point sources on A and B are written

$$\begin{cases} \frac{1}{2\pi}\sigma^a_A(\varphi) = \Sigma^2_e(\varphi)\,[\sigma^s_B\, \mathbf{H}_p(B,A).\mathbf{n}_{s,A}], \\ \frac{1}{2\pi}\sigma^a_B(\varphi) = \Sigma^2_e(\varphi)\,[\sigma^s_A\, \mathbf{H}_p(A,B).\mathbf{n}_{s,B}]. \end{cases} \tag{12}$$

Once again, one recognizes the incoming flexural energy flow on both extremities in the terms inside brackets. Substituting expressions (11,12) in equation (5) leads to the transmitted sound energy at any point M.

5. Numerical results

Some comparison calculations have been performed on a 2 m large aluminum plate ($E = 72\,\mathrm{GPa}$, $\rho_s = 2800\,\mathrm{kg\,m^{-3}}$, $\nu = 0.3$), in air ($c_a = 340\,\mathrm{m/s}$, $\rho_a = 1.3\,\mathrm{kg\,m^{-3}}$). The plate is rigidly baffled and simply supported on its edges. The plane sound wave of unit magnitude is incident with the angle $\theta = 45°$. The plate thickness is $h = 3\,\mathrm{mm}$ and the resultant critical frequency in air is $f_c = 4000\,\mathrm{Hz}$. The plate is lightly damped with a loss factor $\eta = 0.5\%$, in order to emphasize effects of radiation on the structural energy losses. The acoustical media are undamped. Both frequency ranges, below and above the critical frequency are investigated.

The reference results are numerical solutions of the equations of motion. Calculations are performed using a boundary integral method for the acoustic energy, coupled with a modal superposition for the structure [12]. For the acoustics, the Green's function used in the related integral equation is the sum of the contributions of the actual source and the image source which accounts for reflection on the baffle. Thus, the Neumann condition is always fulfilled over the baffle and the fictive sources are confined into the structure. Since the plate is simply supported on its edges, the *in vacuo* modes have a known sine shape. The resulting integral equation is solved by dividing the structure in finite collocation elements. The energy flow results are obtained by solving equations (10-12) and substituting the power source values in equations (4) and (5). Both frequency and spatial evolutions of the flexural energy and the transmitted sound energy are carried out. In both cases, energy flow results are compared to third octave band frequency-averaged reference results.

Figure 6 and 7 show the frequency evolutions of the flexural energy, in dB (re $1\,\mathrm{Jm^{-1}}$), in the middle of the structure and the acoustic energy, in dB (re $1\,\mathrm{Jm^{-2}}$), at two points of the acoustical medium. The calculation begins at $800\,\mathrm{Hz}$ and covers four octaves. The abscissa is the frequency normalized by the critical frequency. For both flexural and acoustic energies, the energy flow approach is shown to give a frequency-averaged estimation of the reference result.

For the structure, the separated contributions of free and forced waves are also shown in Figure 6. Energy flow results are in good agreement with the reference ones, meaning that both the excitation and the energy loss effects are

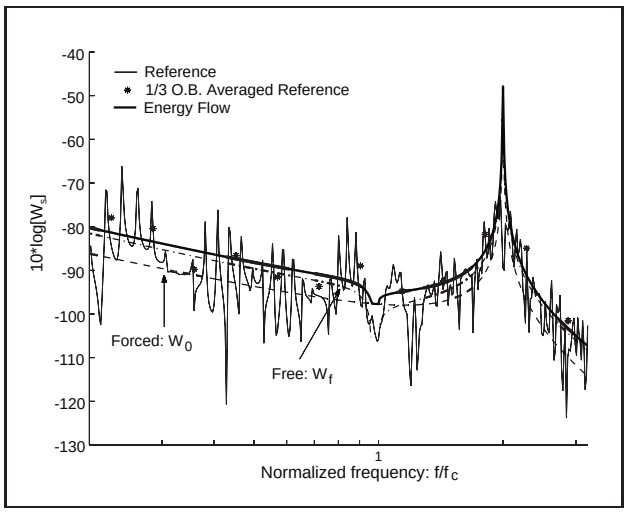

Figure 6. Evolution of the flexural energy in dB ($10 \log W_s$) at the middle point of the structure ($x = 0m$), versus the frequency normalized by the critical frequency. The reference result is plotted in grey, the frequency-averaged reference result with stars and the energy flow result with a thick line. The contributions of the forced and free terms by the energy approach are drawn with dashed lines.

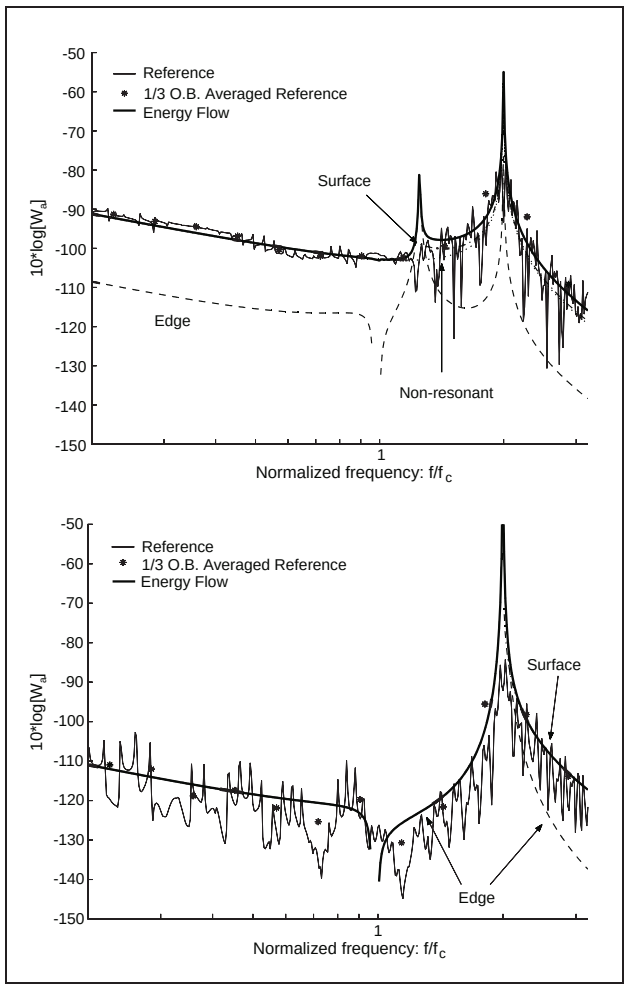

Figure 7. Evolution of the transmitted sound energy in dB ($10 \log W_a$) at two points, versus the frequency normalized by the critical frequency. The reference result is plotted in grey, the frequency-averaged reference result with stars and the energy flow result with a thick line. The contributions of non-resonant transmission, edge radiation and surface radiation, by the energy approach are drawn with dashed lines. Upper: point inside the non-resonant transmission area ($x = 1\,\mathrm{m}$, $y = 1\,\mathrm{m}$). Lower: point outside the non-resonant transmission area ($x = -1\,\mathrm{m}$, $y = 2\,\mathrm{m}$).

well described. The energy approach gives a smooth evolution describing the frequency-averaged reference result. The maximum of energy corresponds to the so-called coincidence frequency ($f_{coin} = f_c / \sin^2\theta = 8000\,\mathrm{Hz}$) where the trace matching of the incoming sound wave occurs [1]. The contribution of the forced wave is shown to be very small except near this coincidence frequency and near the critical frequency. The loss of flexural energy by radiation suddenly increases at the critical frequency, since flexural waves become supersonic. This explains the discontinuity observed on the energy flow results at this frequency. This also explains the fact that the forced contribution becomes here significant.

Concerning the acoustic energy evolution on Figure 7, one point has been chosen inside the non-resonant transmission area, i.e. the beam of transmitted sound by non-resonant effect in the direction of the incoming wave, the other one outside: ($x = 1\,\mathrm{m}$, $y = 1\,\mathrm{m}$) and ($x = -1\,\mathrm{m}$, $y = 2\,\mathrm{m}$) in the frame centered in the middle of the plate (see Figure 1). The contributions of non-resonant transmission, edge radiation and surface radiation given by the energy flow approach are also plotted.

The transmitted energy field is shown to be non diffuse with more than 30 dB between both points at particular frequencies. Here again one can identify the coincidence and critical frequencies. Reference and energy flow results match well except at particular frequencies where energy flow results become very large. They correspond to frequencies for which the point is located near a caustic due to the supersonic waves radiation. Notice that the location of these caustics moves since the radiation angle φ_s^2 from equation (A14) is frequency dependent. When the frequency is such that the caustic goes through the vicinity of the point, the energy flow evaluation is wrong. It happens at $f/f_c = 1.2$ for the first point. The energy at the first point is mainly due to the non-resonant transmission below this frequency. Then, the surface radiation appears, having quite the same contribution than the non-resonant effect. The level of surface radiation is strongly related to the light level of structural damping, inducing a large free field on the structure. For the second point, the main contribution comes from edge radiation in the subsonic frequency range and until $f/f_c = 2$. Then the far more efficient surface radiation appears and edge radiation becomes negligible.

Figures 8 and 9 are concerned with the distributions of flexural and acoustic energies for an excitation below the critical frequency ($f = 3000\,\mathrm{Hz}$, $f/f_c = 0.75$). In Figure 8, the third octave band frequency-averaged reference result and the energy flow result are plotted. The averaged

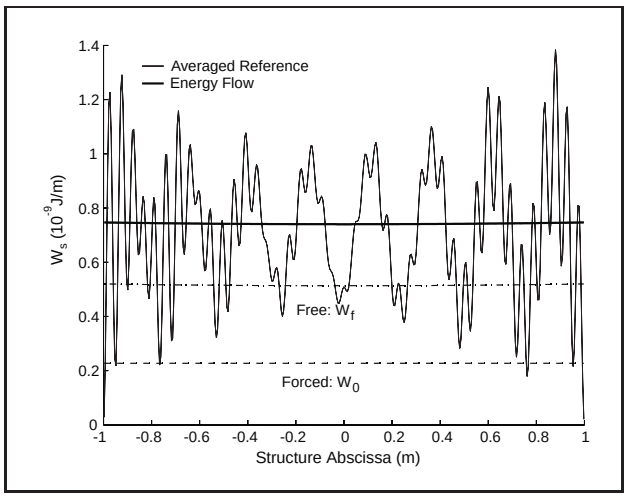

Figure 8. Flexural energy distribution in the structure, for an excitation below the critical frequency ($f/f_c = 0.75$). The frequency-averaged reference result is plotted in grey, the energy flow result with a thick line. Contributions of the forced and free terms by the energy flow approach are drawn with dashed lines.

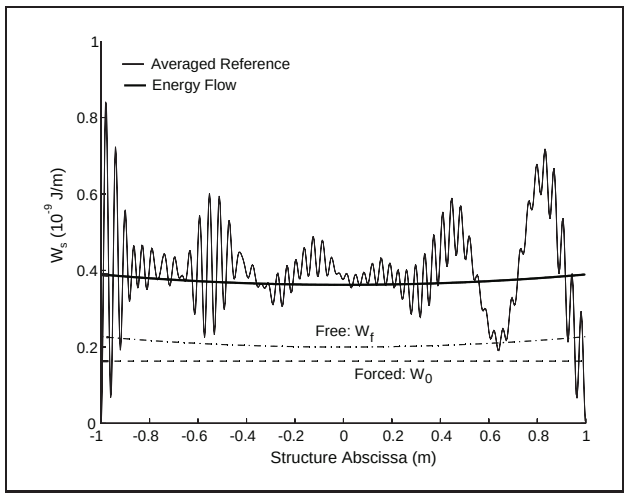

Figure 10. Flexural energy distribution in the structure, for an excitation above the critical frequency ($f/f_c = 1.25$). The frequency-averaged reference result is plotted in grey, the energy flow result with a thick line. Contributions of the forced and free terms by the energy flow approach are drawn with dashed lines.

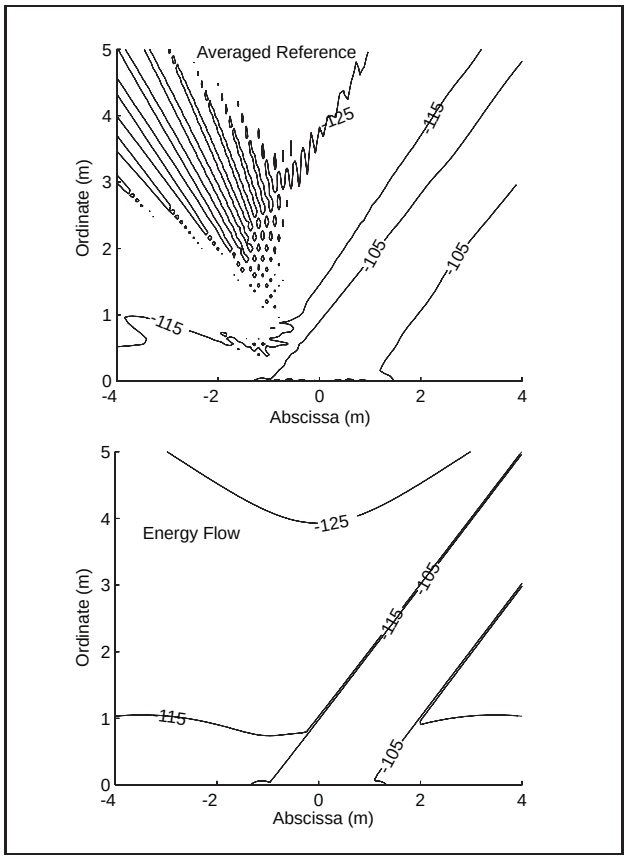

Figure 9. Contour plot of the transmitted sound energy in dB ($10 \log W_a$), for an excitation below the critical frequency ($f/f_c = 0.75$). The plate is located between abscissa -1 m and 1 m on the ordinate 0 m.

flexural energy is shown to have a fluctuating spatial dependence, especially in the vicinity of extremities where the assumption that waves are uncorrelated is not valid. Away from extremities, fluctuations tend to reduce and the energy level is well represented by the sum of the uncorrelated free and forced terms, plotted with dashed lines.

The forced energy is constant along the structure. Energy losses for the free field are due to both the structural damping acting as waves attenuation, and edge radiation effects occurring at the reflection of the flexural waves. Figure 9 shows the maps of the transmitted sound energy by the frequency-averaged reference result in the upper diagram and by the energy flow result in the lower one. Contours are plotted in dB (re $1\,\mathrm{Jm}^{-2}$). The plate is located between abscissa -1 m and 1 m on the ordinate 0 m.

The averaged transmitted energy is shown to be the sum of the uncorrelated effects of non-resonant transmission and edge radiation, except in the vicinity of caustics. These two caustics starting from the extremities of the structure with the angle $\theta = 45°$ are clearly identified as two straight lines. They delimit the sound beam due to the non-resonant transmission. The energy outside this beam is only due to the edge scattering of the flexural free field, which constitutes the resonant transmission.

The same simulation has been performed for an excitation above the critical frequency ($f = 5000\,\mathrm{Hz}$, $f/f_c = 1.25$). The flexural energy distribution along the structure is shown in Figure 10.

Compared with the previous subsonic case in Figure 8, surface radiation effect is now added to the internal damping leading to an increased attenuation of free waves. One may thus observe that the slope of the free energy along the structure is larger in the supersonic case, due to the apparition of these radiation effects. Figure 11 shows the maps of the transmitted sound energy in dB (re. $1\,\mathrm{s\,m}^{-2}$). The energy flow result matches well with the frequency-averaged reference result.

Both effects of non-resonant transmission and supersonic flexural waves radiation are recognized on the radiation pattern. They produce six caustics easily identified.

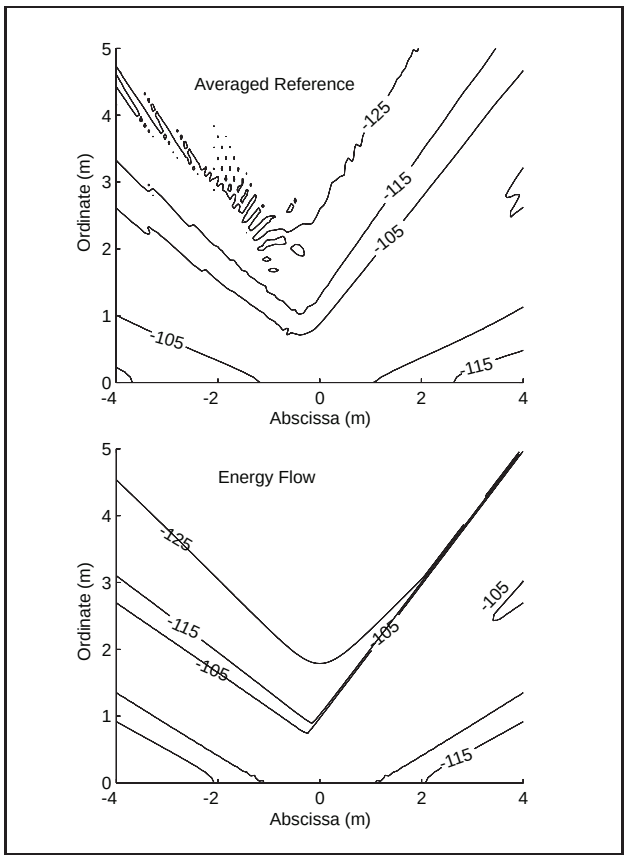

Figure 11. Contour plot of the transmitted sound energy in dB ($10 \log W_a$), for an excitation above the critical frequency ($f/f_c = 1.25$). The plate is located between abscissa -1 m and 1 m on the ordinate 0 m.

The two caustics delimiting the non-resonant transmission beam emanate from the edges with the angle $\theta = 45°$. Four caustics (two directions from both edges) due to the supersonic waves radiation emanate from the edges with the angles $\varphi_s^2 = \pm 63.4°$ given by equation (A14). This radiation process is the main contributor to the resonant transmission. However, edge scattering effects remain significant since they explain the energy level outside the beams due to non-resonant transmission and supersonic radiation.

6. Concluding remarks

An energy flow approach has been extended to sound transmission problems. Both the structure and the acoustical media are described in terms of simple traveling waves. It is shown that the assumption that waves are uncorrelated and the use of the locality principle lead to a simple and intuitive representation of the averaged energy fields. Some power sources are introduced on subsystems boundaries in order to check the local power balance. Averaged energy fields are well described, except in the vicinity of caustics, where the decomposition in uncorrelated simple waves does not apply. The method clearly distinguishes the several contributions to the transmitted sound, i.e. non-resonant transmission, surface radiation and edge radiation.

As SEA, the present approach is dedicated to the high frequency range where the locality principle and the assumption of waves decorrelation are valid. However, no assumption has been made on the vibration fields except the decomposition in simple uncorrelated waves. As a consequence, the approach enables us to describe the distribution of energy, even for non diffuse fields like encountered in exterior radiation and transmission problems. Of course it requires a more precise description of systems and more CPU-time than SEA does, but it still provides a huge gain compared to reference calculations. Both approaches give results to be compared to frequency-averaged data. Notice that due to the wrong description of the acoustic energy in the vicinity of caustics, the method is not suitable for the calculation of the global transmission loss.

The two-dimensional problem studied in this paper was chosen to enable the reference calculations at high frequency. It should be stressed that the method is applicable to three-dimensional geometries, provided the corresponding canonical problems are solved [13].

Appendix

A1. Canonical problems resolution

The canonical problems involved in the transmission of sound are solved below. Since the structure is one-dimensional, the normal incidence of flexural waves is the only to be considered here. In the following equations, we note k_s the flexural wavenumber, c_s the flexural group speed and D the flexural stiffness. Hysteretic damping may be introduced by considering the complex stiffness $D(1 + \mathrm{j}\eta)$, where η is the damping loss factor. k_i, c_i and ρ_i denote the wavenumber, the wave velocity and the density in the acoustical medium i. All calculations are performed under harmonic conditions and the time factor $\mathrm{e}^{\mathrm{j}\omega t}$ is omitted.

A1.1. Non-resonant transmission

Given an infinite plate excited by a plane sound wave incident with the angle θ from medium 1, $p(x,z) = p_0\, \mathrm{e}^{-\mathrm{j}\, k_1 (\sin\theta\, x + \cos\theta\, z)}$, a plane sound wave is reflected in medium 1 and transmitted in medium 2 (Figure 2). The ratios of reflected and transmitted powers over the incident one are written in terms of the plate and acoustical media impedances as

$$\Sigma_{nr}^1(\theta) = \left| 1 - \frac{2\,Z_1}{Z_s + Z_1 + Z_2} \right|^2 \qquad \text{(A1)}$$

$$\text{and} \qquad \Sigma_{nr}^2(\theta) = \frac{Z_1}{Z_2} \left| \frac{2\,Z_2}{Z_s + Z_1 + Z_2} \right|^2 ,$$

where $Z_i = -j\,\rho_i \omega^2 / k_i \cos\varphi_{nr}^i$, and $Z_s = D(k_s^4 - k_1^4 \sin^4\theta)$. The corresponding directivities are derived by applying the Snell-Descartes law for reflection and transmission. The reflection and transmission angles are ex-

pressed in terms of the incidence angle and the wavenumbers as follows:

$$\varphi_{nr}^1 = \theta \quad \text{and} \quad \sin\varphi_{nr}^2 = \frac{k_1}{k_2}\sin\theta. \tag{A2}$$

The forced transverse displacement of the structure is written

$$u_0\,\mathrm{e}^{-\mathrm{j}\,k_1\sin\theta\,x} \quad \text{with} \quad u_0 = 2p_0/(Z_s + Z_1 + Z_2). \tag{A3}$$

The corresponding time-averaged energy W_0, is the sum of the kinetic and potential energies,

$$W_0 = \frac{1}{4}m_s\omega^2|u_0|^2 + \frac{1}{4}\Re[D](k_1\sin\theta)^4|u_0|^2, \tag{A4}$$

where m_s is the mass per unit of area of the plate and $\Re$ denotes the real part. Notice that for forced displacements, kinetic and potential time-averaged energies are not equal. Expressing the incident sound power $P_{inc} = |p_0|^2\cos\theta/2\rho_1 c_1$, and substituting (A3) in (A4) leads to the expression of the flexural energy in terms of the incident power,

$$W_0 = \left(m_s\omega^2 + \Re[D](k_1\sin\theta)^4\right) \frac{2|Z_1|}{\omega\left|Z_s + Z_1 + Z_2\right|^2}P_{inc}. \tag{A5}$$

The power being dissipated by structural damping is written $P_{diss} = P_{inc}(1 - \Sigma_{nr}^1 - \Sigma_{nr}^2)$. Calculations enable to check that it is related to the potential energy V_0 and the hysteretic loss factor η by the equality $P_{diss} = 2\eta\omega V_0$. Since the potential energy is proportional to the incident power, we may write $P_{diss} = \Sigma_{nr}^{diss}P_{inc}$ with

$$\Sigma_{nr}^{diss} = \frac{4|Z_1|\Re[D](k_1\sin\theta)^4}{\left|Z_s + Z_1 + Z_2\right|^2}\,\eta. \tag{A6}$$

A1.2. Excitation of structures

Given a semi-infinite plate excited by plane sound wave in medium 1 (Figure 3), we seek to determine the power supplied to the plate. Following the approach of reference [1], one may evaluate the free displacement field that checks the boundary conditions of the plate with the forced displacement field, assuming that the fluid loading is negligible. Compared to the previous canonical problem, the plate is now bounded on the abscissa $x = 0$, which explains the presence of the structural free field.

The expression of the forced displacement is given in equation (A3). The free structural waves in the *in vacuo* plate have the wavenumbers k_s and jk_s. By expressing the boundary conditions involving the forced wave and both propagative and evanescent free waves, the magnitude of each free wave may be obtained. For example, for simply supported boundary conditions ($u = 0$ and $d^2u/dx^2 = 0$ on abscissa $x = 0$), the magnitude of the propagative free wave is written $u_{pr} = u_0[1 - (k_1\sin\theta/k_s)^2]/2$. Since evanescent waves do not carry power away from the boundary, they are not accounted in the evaluation of the transmitted power, and the propagative wave is the only one to be considered here. The power carried by this wave is the sum of transverse and rotation velocities effects,

$$P_s = \frac{\omega}{2}\,\Re\left[D(k_s^3 + k_s^2\,k_s^*)\right]|u_{pr}|^2, \tag{A7}$$

where * denotes the complex conjugate. Σ_r is the ratio of this power P_s over the incident sound power P_{inc},

$$\Sigma_r = \frac{P_s}{P_{inc}} = \frac{\mathrm{j}Z_1\,\Re\left[D(k_s^3 + k_s^2\,k_s^*)\right]}{\left|Z_s + Z_1 + Z_2\right|^2} \left|1 - \left(\frac{k_1\sin\theta}{k_s}\right)^2\right|^2. \tag{A8}$$

A1.3. Radiation of flexural waves by edge scattering

The sound power radiated when a flexural wave is reflected on the extremity of a plate (Figure 4) is calculated as follows: considering that the fluid loading is light, the radiated pressure is expressed using spatial Fourier transforms of the *in vacuo* velocity field [10].

Consider a rigidly baffled extremity, the negative half-space ($x < 0$) corresponding to the wave bearing structure. A flexural wave of unit displacement magnitude is incident on the edge. If v^- denotes the reflected transverse velocity on $x < 0$ and v^+ the velocity field on $x > 0$ corresponding to the incident wave traveling without the edge discontinuity, we note V the Fourier transform of the following field:

$$\begin{cases} v^-(x) & x < 0, \\ -v^+(x) & x > 0. \end{cases} \tag{A9}$$

The corresponding radiated pressure in medium i is written with the inverse Fourier transform

$$p_i(x,z) = \int_{-\infty}^{+\infty} \frac{\rho_i\omega\,V(\gamma)}{(k_i^2 - \gamma^2)^{1/2}}\mathrm{e}^{-\mathrm{j}(\gamma x + \sqrt{k_i^2-\gamma^2}z)}\,\mathrm{d}\gamma. \tag{A10}$$

The diffracted pressure corresponds to the branch cut contribution of integral (A10). It is evaluated by the stationary phase approach and the far-field pressure is expressed in cylindrical coordinates r, φ defined by $x = r\cos\varphi$,

$$p_i(r,\varphi) = -\rho_i\omega\sqrt{\frac{2\pi}{k_i r}}V(k_i\cos\varphi)\,\mathrm{e}^{-\mathrm{j}\,(k_i r + \pi/4)}. \tag{A11}$$

The resulting time-averaged sound intensity is written $|p_i(r,\varphi)|^2/2\rho_i c_i$. Divided by the incident flexural power expressed with equation (A7) for a wave of unit magnitude, we get the ratio Σ_e^i of sound power radiated in an unit solid angle around φ over the incident structural power,

$$\Sigma_e^i(\varphi) = \frac{2\pi\rho_i|V(k_i\sin\varphi)|^2}{\Re\left[D(k_s^3 + k_s^2\,k_s^*)\right]}. \tag{A12}$$

This power was calculated using the *in vacuo* flexural displacement field for which no power is actually loss by radiation. Consequently, the amount of flexural energy re-

flected by the edge when the plate is loaded by a fluid must account for this effect. In order to respect the power balance at the edge, the *in vacuo* energy reflection coefficient R_{vacuo} must be changed to R by taking into account the radiated power on both sides,

$$\frac{R}{R_{vacuo}} = 1 - \int_{-\pi/2}^{\pi/2} \left[\Sigma_e^1(\varphi) + \Sigma_e^2(\varphi)\right] \, \mathrm{d}\varphi. \quad \text{(A13)}$$

A1.4. Radiation of supersonic flexural waves

A simple calculation using the propagative forms of the flexural and sound waves for an infinite fluid-loaded plate shows that radiation occurs when flexural waves are supersonic (Figure 5). A traveling sound wave is radiated in each medium i. This wave is shown to propagate with the angle

$$\varphi_s^i = \arcsin(\Re[k_s]/k_i) \quad \text{(A14)}$$

with the normal to the plate. Noting $K_i = (k_i^2 - k_s^2)^{1/2}$, the ratio of radiated power over the flexural power is written

$$\Sigma_s^i = \frac{\rho_i \omega^2 \, \Re[K_i]}{|K_i|^2 \, \Re\left[D\,(k_s^3 + k_s^2\, k_s^*)\right]}. \quad \text{(A15)}$$

The resulting attenuation on the flexural waves is expressed in terms of the group velocity of flexural waves c_s, by the loss factor $\eta_s = c_s(\Sigma_s^1 + \Sigma_s^2)/\omega$, taking into account the radiation on both sides of the plate.

Acknowledgment

This work was supported by Dassault Aviation (France) and by a Lavoisier fellowship of the Ministère des Affaires Étrangères Français.

References

[1] M. Heckl: The tenth sir Richard Fairey memorial lecture: sound transmission in building. J. Sound Vibr. **77** (1981).

[2] M. J. Crocker and A. J. Price: Sound transmission using statistical energy analysis. J. Sound Vibr. **9** (1969).

[3] R. H. Lyon and R. G. DeJong: Theory and applications of statistical energy analysis. Butterworth-Heinemann, USA, 1995.

[4] H. Kuttruff: Energetic sound propagation in rooms. Acustica **83** (1997).

[5] A. Le Bot: A vibroacoustic model for high frequency analysis. J. Sound Vibr. **211** (1998).

[6] A. Le Bot and A. Bocquillet: Comparison of an integral equation on energy and the ray-tracing technique in room acoustics. J. Acoust. Soc. Am. **108** (2000).

[7] F. Bitsie and R. J. Bernhard: Structure-borne noise prediction using an energy finite element method. Proc. Noise and Vibration Conference - Society of Automotive Engineers, 1997.

[8] V. Cotoni and A. Le Bot and L. Jezequel: High-frequency radiation of L-shaped plate by a local energy flow approach. J. Sound Vibr. **250** (2002).

[9] D. Bouche and F. Molinet and R. Mittra: Asymptotic methods in electromagnetics. Springer-Verlag, 1997.

[10] D. G. Crighton: Acoustic edge scattering of elastic surface waves. J. Sound Vibr. **22** (1972).

[11] G. Maidanik: Response of ribbed panels to reverberant acoustic fields. J. Acoust. Soc. Am. **34** (1962).

[12] P. M. Morse and K. U. Ingard: Theoretical acoustics. Princeton University Press, 1986, page 375.

[13] V. Cotoni and A. Le Bot and L. Jezequel: High frequency plate radiation by power flow analysis with experimental validation. Proc. Inter.Noise 2000 - Nice, 2000.